

# Groundwater Prospecting and Exploration in a Low Potential Hard Rock Aquifer: Case Study from Ogbomoso North, South-western Nigeria

Oladunjoye Michael<sup>1</sup>, Adabanija Moruffdeen<sup>2\*</sup>, Adebayo Oni<sup>1</sup>

<sup>1</sup>Department of Geology, University of Ibadan, Ibadan, Nigeria

<sup>2</sup>Department of Earth Science, Ladoke Akintola University of Technology, Ogbomoso, Nigeria

\* E-mail of the corresponding author: [maadabanija@lautech.edu.ng](mailto:maadabanija@lautech.edu.ng)

## Abstract

Very Low Frequency Electromagnetic (VLF-EM) and Electrical Resistivity methods has been employed to unravel the localized nature of groundwater occurrence in Ogbomoso North, southwestern Nigeria. This was aimed at addressing the growing demand for groundwater use in the area underlain by migmatite gneiss with minor intrusions of pegmatite and quartz veins.

Nine profiles comprising five VLF-EM and four electrical resistivity profiles were conducted parallel to the two major azimuths in the area. The anomalous zones identified on the profiles were further investigated by twelve Vertical Electrical Soundings (VES). Lithologic logs from three boreholes were also used to ground truth the geophysical findings.

Quantitative interpretation of VES data showed that the Geoelectrical Succession comprise three to five layer earth models. The aquifer units are localized comprising weathered layer and fractured basement. The lowest yield of 280.6LPH was obtained from well bored on VES point having three-layer earth models made up of *resistive-conductive-resistive* geoelectric succession. Well bored on VES points having more than three-layer earth models and comprising alternating band of *resistive-conductive* geoelectric succession have more yield ranging between 520.8LPH and 590.4LPH. Furthermore, there was strong correlation between geoelectric succession and lithologic sections obtained from the drill cuttings of the bored wells.

**Keywords:** Groundwater Exploration, Geophysical Methods, Lithology Logs, Fractured Basement, Crystalline Rocks.

## 1. Introduction

The basement complex rocks of Nigeria occupy about 50% of the total area where over 40% of the rural populace reside. The crystalline rocks have low primary porosity and relatively impermeable and have therefore previously been thought to be poor aquifers, non-productive or with limited groundwater yield (Ajayi and Adegoke Anthony, 1988). Hence, the occurrence and distribution of groundwater in crystalline rock units are controlled by the presence and development of integrated fracture system, the intensity of fracturing and weathering. Thus, the occurrence of groundwater in the basement terrain is localized and concentrated within two major zones; the weathered layer/regolith and the fractured underlying rock unit. The search for water in both zones had to rely on detailed geological knowledge and application of geophysical techniques to locate these targets. This is in effect to minimize the present net cost of water supply while ensuring production of high quality and quantity water resources. The combination of Electromagnetic Method (EM) and Vertical Electrical Sounding (VES) had proved to be the most effective in this regard and is becoming a standard method of exploration to locate and evaluate regolith and fracture aquifers in basement complex (Jones, 1985; Jones and Beeson, 1985; Beeson and Jones, 1988; Palacky *et al.*, 1981; Reynolds, 1987; Hazell *et al.*, 1988). For instance in Crystalline Basement of Northern Nigeria, the combined methods have been used to deduce resistivity/conductivity criteria related to lithology and weathering by Beeson and Jones (1988) and Hazell *et al.*, (1988). This has made it possible to drill rapidly into hard rock and to intersect fractures with excellent yield. These methods have also been successfully used to locate conductive zones in some part of Africa (Beeson and Jones, 1988; Hazell *et al.*, 1988; Payne, 1988; Amadi and Nurudeen, 1990; Olayinka, 1990; Goldman *et al.*, 1994, Olorunfemi *et al.*, 2000).

The present study involves the combined use of VLF-EM and electrical resistivity methods to identify and characterize the hydro-geological potential of Ogbomoso Northeast, a semi-urban settlement in Southwestern Nigeria basement complex. The study is necessitated by the perennial water scarcity facing

the residents of the area especially during the dry season. This is in addition to increase in population as a result of the siting of a state University, Ladoke Akintola University of Technology (LAUTECH); Bowen University Teaching Hospital; and Baptist Theological Institute in the area. Hence the objectives of the study are: delineation of the conductive zones and/ or fractured zones saturated with water; efficacy and evaluation of the combined use of VLF-EM and electrical resistivity method in locating suitable sites for water borehole drilling.

The significance of using VLF-EM is the quick identification of high conductivity anomalies thought to be due to deep weathering and/or fractured zones saturated with water. This is accomplished using EM profiling which enables the determination of the qualitative picture of the subsurface conductivity structure. Such anomalies are further ascertained and evaluated for their groundwater potential using conventional electrical resistivity methods employing horizontal profiling and Schlumberger Vertical Electrical Sounding (VES). This provides more quantitative information of the subsurface through the geo-electrical profile of the weathered/fractured zone. A preliminary hydro-geological assessment of the study area shows that the average total depth of hand-dug wells are less than 6 m and most of them are resting on the basement rock indicating shallow overburden.

## 2.0 Location, Geologic and Hydrogeologic Setting

Ogbomoso is located in the southwestern part of Nigeria. It lies between latitudes  $8^{\circ} 05'N$  and  $8^{\circ} 11'N$  and longitudes  $4^{\circ} 12'E$  and  $4^{\circ} 19'E$  (Figure 1). The terrain in Ogbomoso area is gently undulating with sub-dendritic drainage pattern (Figure 2). The climate is characterized by alternation of wet season lasting from April to October and dry season from November to March.

The study area is geologically located within the southwestern Nigeria basement complex. The rocks unit made up of ancient gneiss-migmatite series and meta-sedimentary series (Afolabi *et al.*, 2013). The former series is represented by gneisses occurring mainly as granite gneiss (Figure 3) with medium to coarse-grained textures and no definite foliation pattern. They contain biotite, hornblende, quartz, plagioclase, microcline and rarely pyroxene. Those gneisses with high content of mafic minerals may yield clayey soils while the coarse grained, more granitic components may account for soils with varying textures with less clay (Afolabi *et al.*, 2013).

The meta-sedimentary series include quartzite and quartz-schists. The quartzite occur as long elongated ridges trending NW-SE and mostly massive schistose quartzites with micaceous minerals alternating with quartzo-feldspathic rocks which are common in the southwestern part of Ogbomoso (Figure 3). The integrated, network of fractures, joints and plane of schistosity present in quartzites enhances weathering process.

The older granites consist of medium to coarse-grained porphyritic granites, granodiorites, biotite granites and affiliated minor rocks such as pegmatites. Pegmatites are common as intrusive rocks occurring as dykes filling the shear and joints. They are coarse grained and weathered easily to clay and sand size particles, which serve as water bearing horizon of the regolith.

The weathered profiles developed over the basement rocks is relatively shallow and corroborated by shallow hand-dug wells (depth less than 5m) resting directly on the basement rocks within the vicinity of the survey area. The direction of groundwater flow in Ogbomoso area is predominantly southward and westward (Figure 4) and structurally controlled with the study area lie within groundwater recharge.

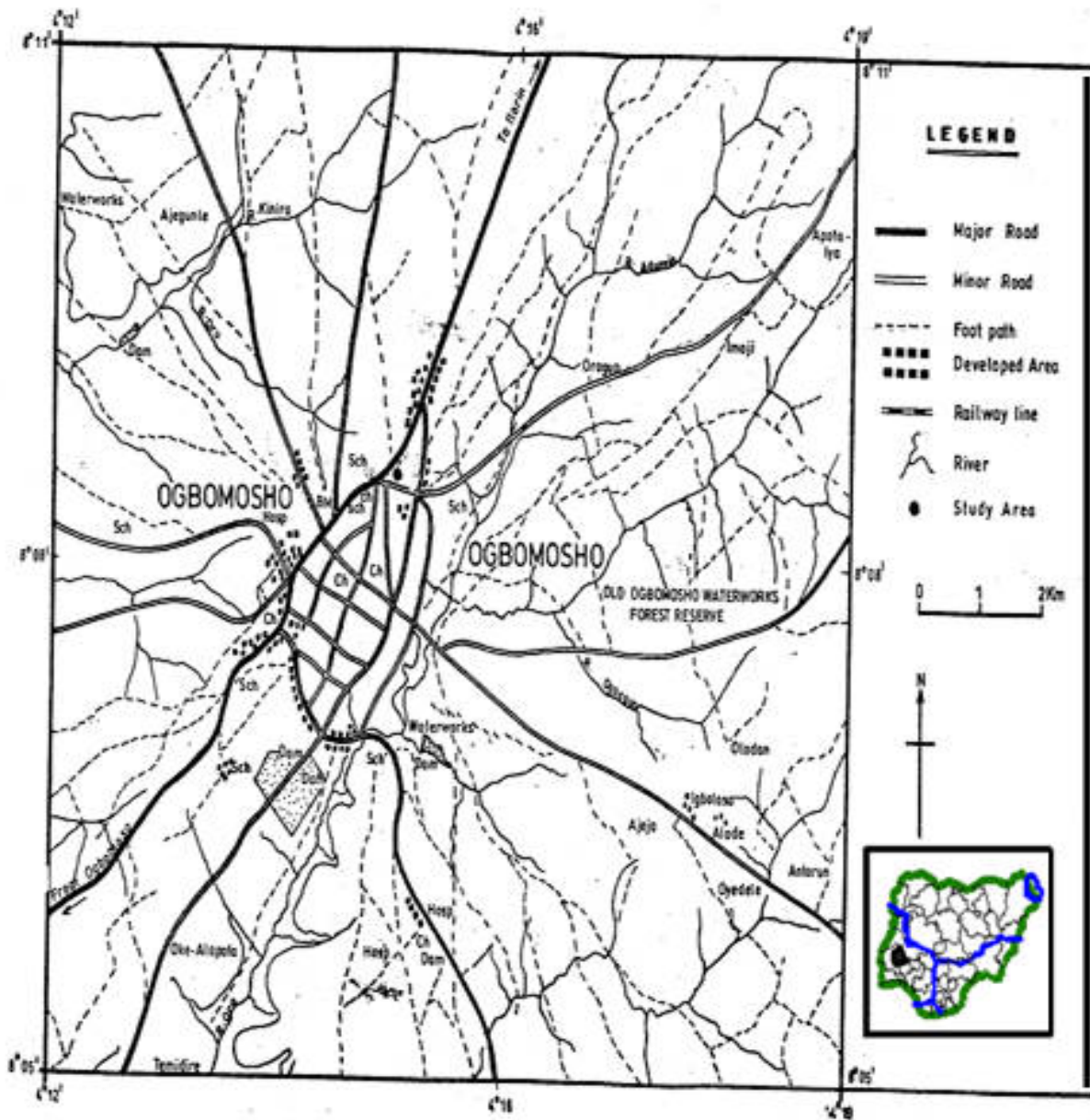


Figure 1. Map of Ogbomosho showing the location of study area

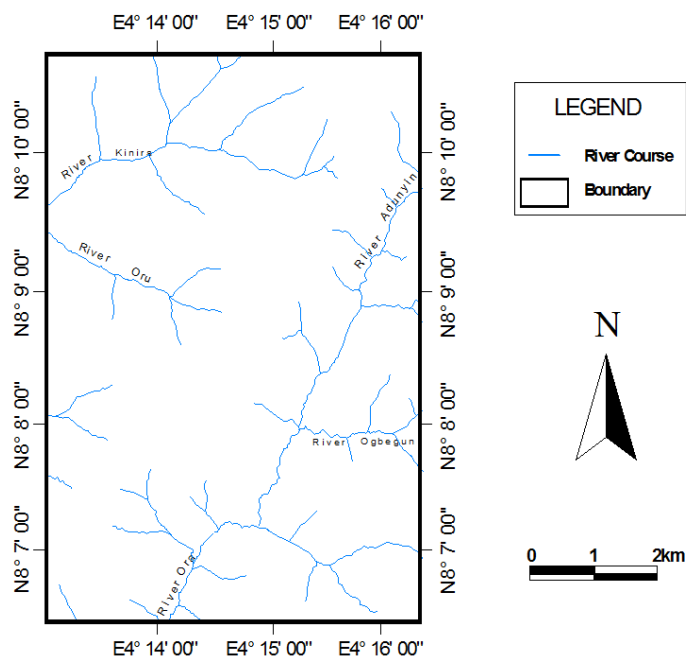


Figure 2. Map showing the drainage pattern of Ogbomosho

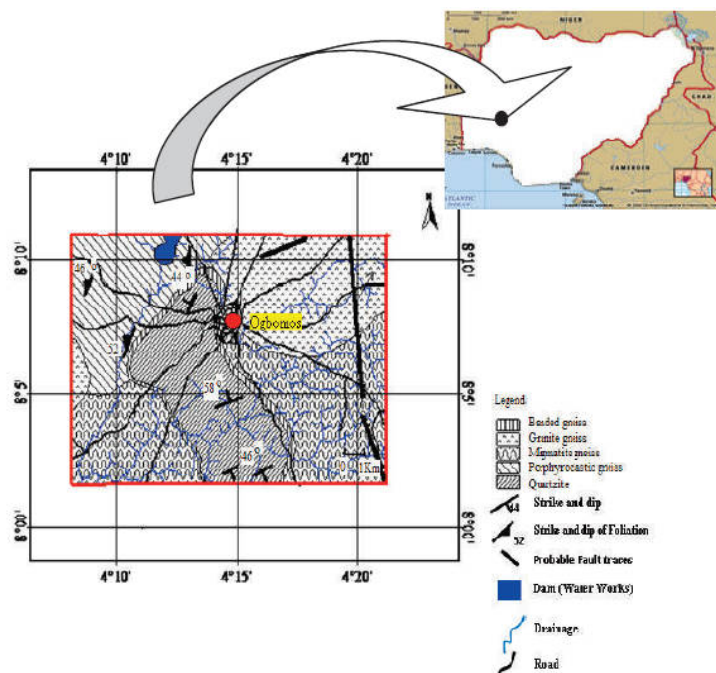


Figure 3. Geological map of Ogbomosho area (after Afolabi et al., 2013)

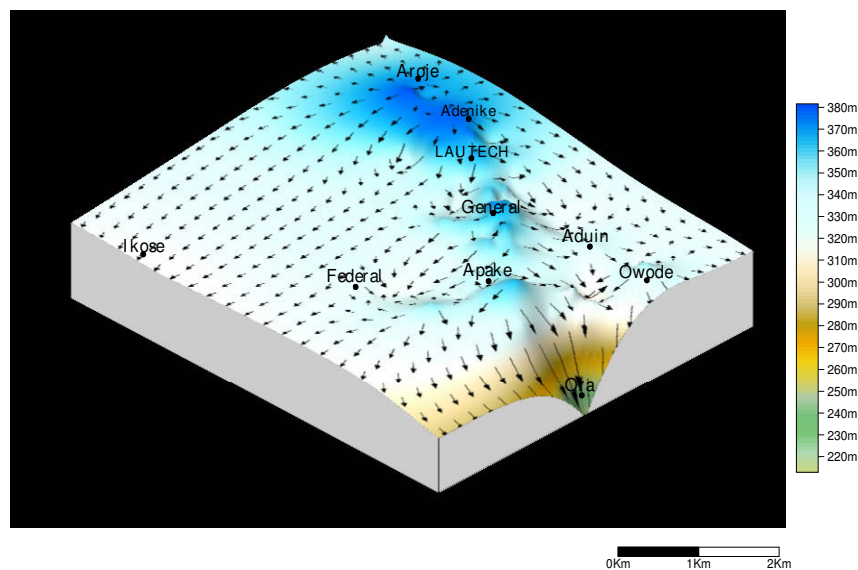


Figure 4. Groundwater flow map of Ogbomoso area, South-western Nigeria

### 3.0 Methodology

#### 3.1 Geophysical Investigation

##### 3.1.1 Very Low Frequency Electromagnetic (VLF-EM) Survey

Electromagnetic method involves the propagation of continuous wave or transient electromagnetic fields into the earth. The electromagnetic fields are of two types namely the primary and secondary electromagnetic field. The primary electromagnetic fields travel from the transmitter coil to the receiver coil via paths both above and below the surface (Figure 5). Where the surface is homogeneous, there is no difference between the field propagated above the surface and through the ground other than a slight reduction in amplitude of the latter with respect to the former. However, in the presence of a conducting body, the magnetic component of the electromagnetic field penetrating the ground induces alternating currents or eddy currents to flow in the conductor. The eddy currents generate their own secondary electromagnetic field which travels to the receiver (Figure 5). The receiver then responds to the resultant of the arriving primary and secondary fields so that the response differs in both phase and amplitude from response to the primary field alone. These differences between the transmitted and the received electromagnetic fields reveal the presence of the conductor and provide information on its geometry and electrical properties.

The existence of the secondary field may be established with respect to primary field by a change of amplitude and phase in the normal detector signal. There is always a phase difference of  $[(\pi/2) + \varphi]$  between the primary and secondary fields (Figure 6). The lag in phase of  $\pi/2$  is attributable to the inductive coupling between transmitter and conductor while the additional phase lag  $\varphi$  is determined by the properties of the conductor as an electric circuit. From Figure 6, the phase difference ( $\theta_p - \theta_s$ ) between primary field  $H_p$  and secondary field  $H_s$  can be expressed as

$$\theta_p - \theta_s = [(\pi/2) + \varphi] \quad (1)$$

For a good conductor,  $\varphi = \pi/2$  and hence

$$\theta_p - \theta_s = \pi \quad (2)$$

For a very poor conductor,  $\varphi = 0$  and hence

$$\theta_p - \theta_s = \pi/2 \quad (3)$$

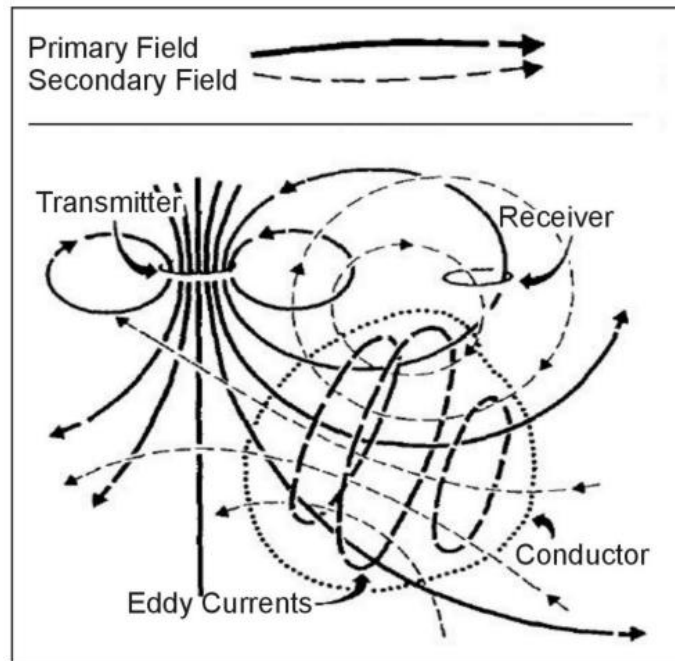


Figure 5. Principle of Electromagnetic prospecting method (adapted from Klein and Lajoie, 1980)

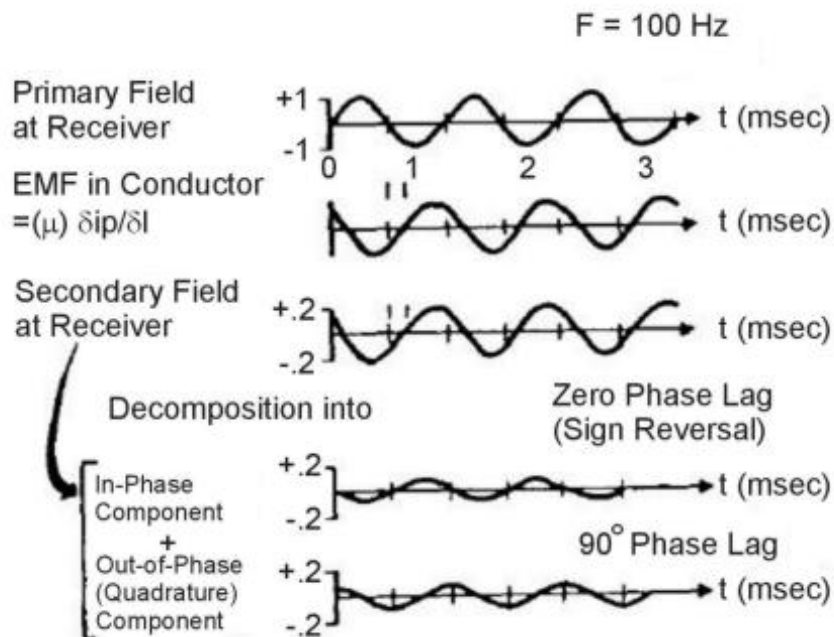


Figure 6. In-phase and out-of-phase component of frequency domain Electromagnetic method (adapted from Klein and Lajoie, 1980)

Equation (2) implies  $H_s$  lagging behind  $H_p$  or  $H_p$  is leading  $H_s$  or  $H_s$  is out-of-phase with  $H_p$  whilst equation (3) implies  $H_p$  and  $H_s$  are in-phase and measured as imaginary and real component respectively on the field. The ratio of  $H_s$  to  $H_p$  is usually expressed as

$$\frac{H_s}{H_p} = \frac{i\omega\mu_0\sigma s^2}{4} \quad (4)$$

yielding the apparent conductivity

$$\sigma_a = 4 \frac{(H_s / H_p)}{\mu_0 \omega s^2} \quad (5)$$

where  $H_s$  is the secondary magnetic field at the receiver coil;

$H_p$  is the primary magnetic field at the receiver coil;

$\omega = 2\pi f$ ;

$f$  is the frequency;

$s$  is the inter-coil spacing in metres;

#### VLF-EM survey

The VLF-EM survey in this study utilizes the ABEM WADI receiver to probe the subsurface geological conditions of the study area. The low frequency field that was used, was sent out from military radio transmitter located at the frequency between 15 and 30 KHz with a very powerful signal of about 300-1000KW (Telford *et al.*, 1990). A profiling technique was employed and traversing was done parallel to the two major azimuths with station separation of 20m along each profile were conducted. A total of 5 profiles were traversed comprising 3 profiles in East-West direction and 2 in a north-south direction (Figure 7). At each location, the *In - Phase* (IP) or real component and the corresponding *Out - of - Phase* (OP) or imaginary components of secondary magnetic field were recorded. The ratios of OP/IP in percentage were plotted against station separation and the profiles obtained were qualitatively interpreted.

Qualitative interpretation involved visual inspection of the profiles by identifying anomalous peaks defined on the profiles and interpret the varying amplitude which measure the conductivity changes in the subsurface. The anomalous peaks identified on the profiles were chosen as targets for electrical resistivity survey, specifically Vertical Electrical Sounding.

#### 3.1.2 Electrical Resistivity Survey

Earth materials have different electrical properties. The variations in these properties are useful geophysical parameters for characterizing earth materials. These electrical properties can be expressed in terms of electrical resistivity  $\rho$  defined in terms of resistance  $R$  of a unit length  $l$  of wire having a unit cross sectional area  $A$ , that is

$$\rho = \frac{RA}{l} \quad (6)$$

The resistance  $R$  is usually determined using Ohm's law  $\Delta V = IR$  by putting a direct current of strength  $I$  into the ground by means of two point electrodes (current electrodes) and measuring the resulting voltage drop  $\Delta V$  between another two points electrodes (potential electrodes) on the ground surface. Equation (6) is therefore the basis of the electrical resistivity method. The electrodes are usually arranged in such a way that at different measurements, the value of the measured potential difference is affected by the formation resistivities at different depth range. This is attained by

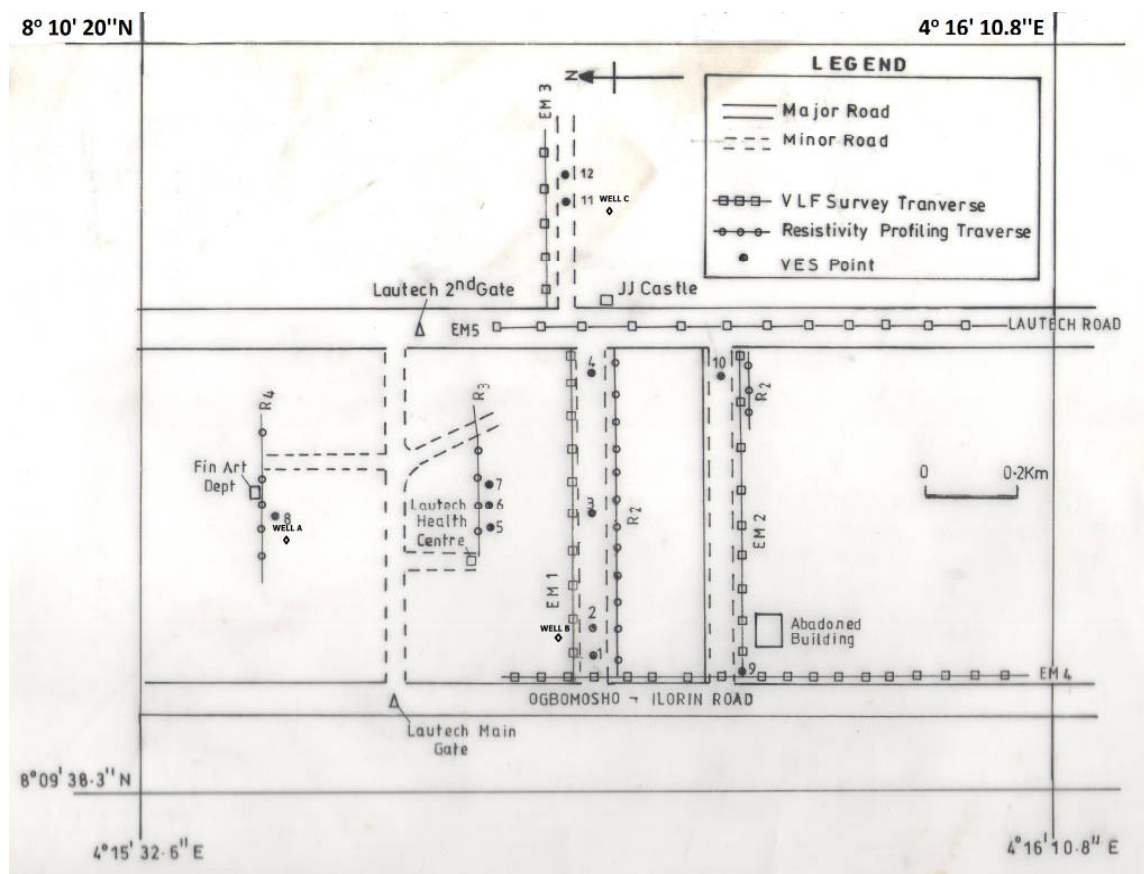


Figure 7. Map showing VLF, Resistivity profile lines and VES points

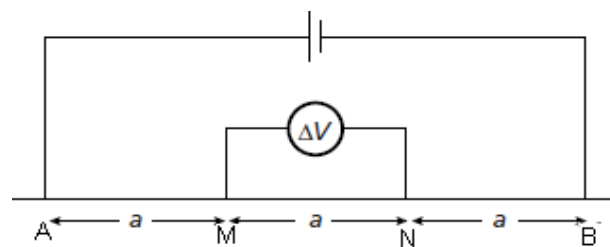
changing the distance between the potential measuring electrodes and their position with respect to current electrodes. Resistivity surveys are therefore conducted using different electrode arrays, for different specific objectives, including depth sounding or Vertical Electrical Sounding, lateral profiling or Constant Separation Traversing (CST) or a combination of the two. As a result of different logistic array (Figure 8), equation 6 can be re-written by incorporating geometric factor K as

$$\ell_a = KR \quad (7)$$

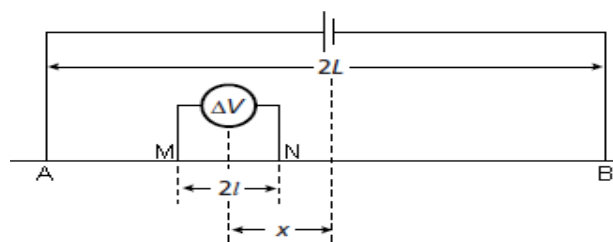
where  $\ell_a$  is the apparent resistivity.

In this study, Electrical Resistivity survey involving Horizontal Resistivity Profiling and Vertical Electric Sounding (VES) was carried out to corroborate the results obtained on EM profiles using Geopulse Campus Tiger Resistivity Meter which measures resistance value at each sampling point with observational error less than 1% in most cases. The horizontal profiling measures the lateral variation in resistivity along selected traverses T1, T2, T3 and T4 (Figure 7). The first two traverses - T1 and T2- were conducted parallel to two respective VLF-EM profiles EM1 and EM2, and the other two were independent (Figure 7). A Wenner electrode configuration ( $AM = MN = NB = a = 20$  m, electrode spacing; Figure 8a) was used for this purpose. Successive measurements were taken at 5 m intervals along profiles T1, T2, T3 and T4. The observed apparent resistivity values obtained from equation (7) were plotted against station distance as electrical resistivity profiles. Points of relatively abnormally low resistivities were considered anomalous and further probed using VES.

A collinear expanding Schlumberger array (Figure 8b) of current electrodes together with fixed potential electrodes was used for VES. In all, twelve sounding points were located and occupied with current electrode separation of 266 m. Analysis of the resulting graph of apparent resistivity versus current half-space separation yields a layered earth model composed of individual layers of specified thickness and resistivity. This was achieved by partial curve matching with sets of auxiliary charts and computer aided iteration (Ghosh, 1971 and Zohdy *et al*, 1974).



(a)



(b)

Figure 8. Symmetric electrode array configuration. (a) Wenner Electrodes array, (b) Schlumberger Electrodes array (Modified from Keary et al., 2002)

#### 4.0 Results and Discussion

##### 4.1 VLF-EM Profiles

The observed VLF-EM field profiles, EM1, EM2, EM3, EM4 and EM5 are as shown on Figures 9a, 9b, 9c and 9d. Profiles EM1, EM2 and EM3 trend approximately in east – west, while profiles EM3 and EM4 are north – south (Figure 7). These relative positions are used in their descriptions.

##### 1. East – West EM Profiles

Generally, changes in subsurface conductivity changes vary from 25% - 40% for profile EM1 (Figure 9a); 15% - 21% for profile EM2 (Figure 9b); and 66% - 76% for profile EM3 (Figure 9c). The anomaly signature showed sharp and broad peak, which is indicative of the depth of burial of the conductive zones. The deeper anomaly peaks are wider and have lower amplitudes. However, the shallower anomaly peaks are narrow and have higher amplitudes (McNeil, 1980, 1990).

In Figure 9a, the OP component showed maximum negative peak at distance of 100 m and 500 m indicating probably weathered layer with a moderate overburden, whereas broad anomaly at distance of about 380 m indicate thick overburden and is as corroborated by IP component with positive real amplitudes percentage change of about 3%. The IP component also indicated moderately thick overburden at distance of about 580 m. The coincidence of arrival of both IP and OP peaks at these

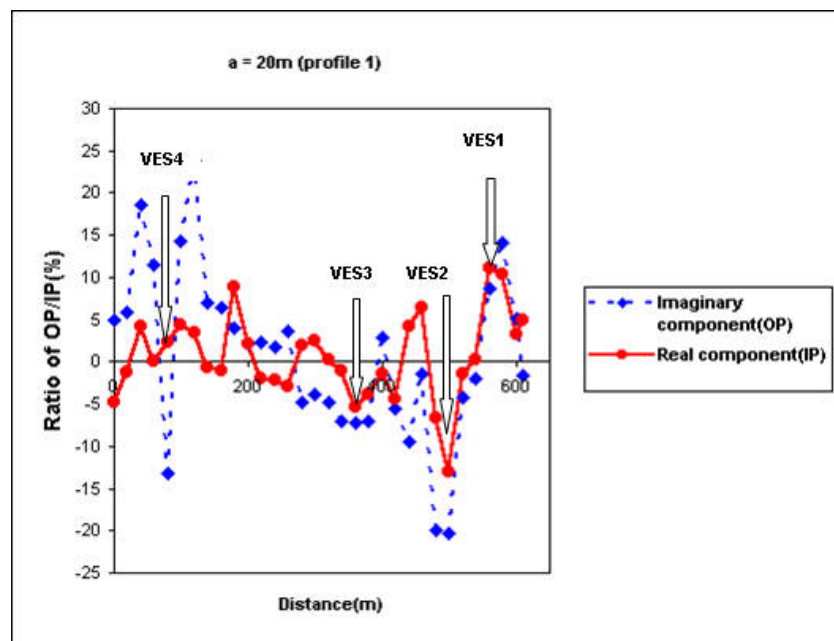


Figure 9a. Profile VLF-EM1 along E-W direction of the study area distances implied anomalies and were subjected to investigation using VES (VES1, VES2, VES3 and VES4).

In Figure 9b, profile EM2 showed two pronounced anomalies with peak negative imaginary and peak positive real amplitudes at distance of about 450 m and 600 m. These probably indicate the presence of shallow overburden and fairly good conductive zone at 600 m distance and hence subjected to VES (VES9); and a moderately thick overburden with fairly good conductive zone at 450 m distance.

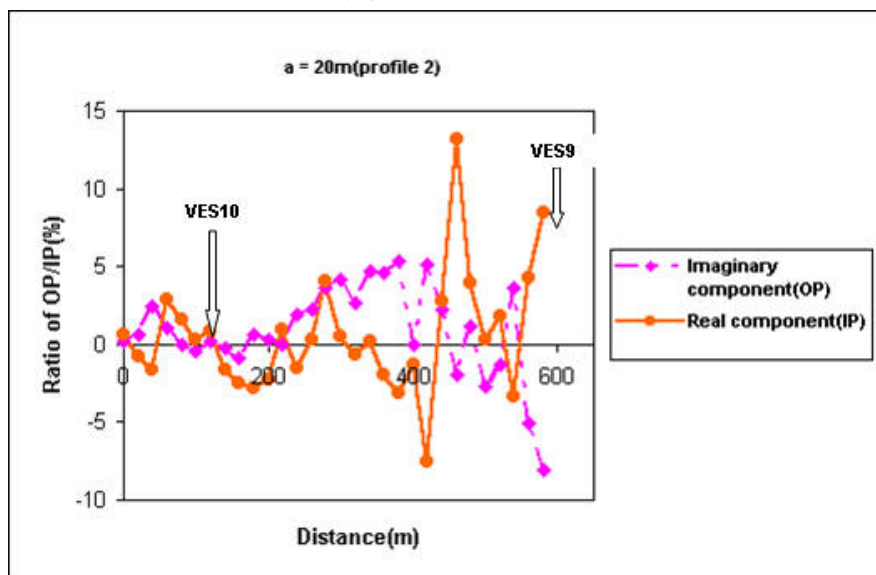


Figure 9b. Profile VLF-EM2 along E-W direction of the study area  
 Profile EM3 (Figure 9c) indicates conductive zone at distance of about 20 m as a result of anomaly caused by peak negative imaginary (about 38%) and peak positive real amplitudes (about 18%) and

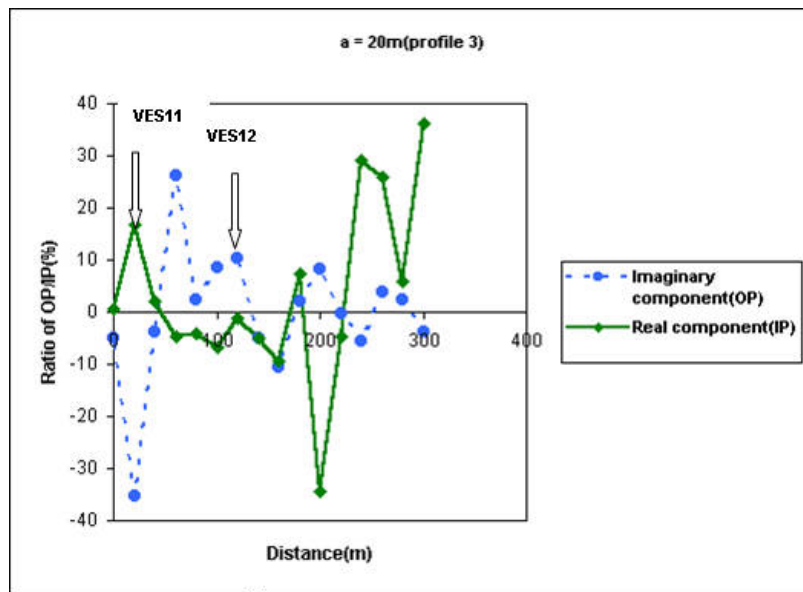


Figure 9c. Profile VLF-EM3 along E-W direction of the study area hence was further investigated using VES (VES11).

## 2 North – South EM Profiles

The North – South EM Profiles comprise EM4 and EM5. The real component signature of profile EM5 (Figure 9d) indicates overburden thickness ranging from moderately thick (at distances of 180 m, 350 m, 700 m and 750 m) to very thick between 550 m and 600 m distance. A notable feature of this signature however is its asymmetric anomaly between 550 m and 850 m. The anomaly is symmetric about 700 m distance mark and indicative of the attitude of the fracture occurring at about 650 m mark.

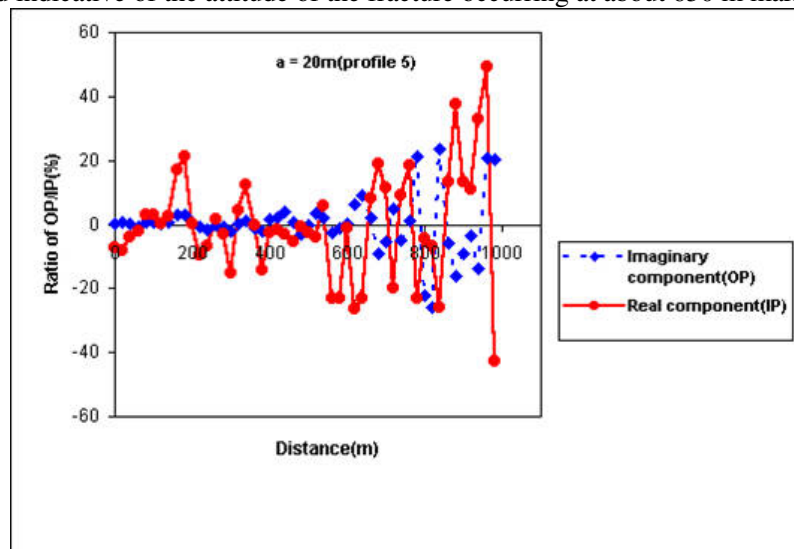


Figure 9d. Profile VLF-EM5 along N-S direction of the study area

## 4.2 Electrical Resistivity Profiles/Sounding

### 4.2.1 Horizontal Resistivity Profiling

The horizontal electrical resistivity profiles are as depicted in Figure 10a, Figure 10b, Figure 10c and Figure 10d for profile T1, T2, T3 and T4 respectively. The interpretations were based on the fact that rocks are poor conductors and will have high resistivity values but their electrical properties are largely due to the amount and quality of their water contents (Oyedele and Momoh, 2009). Hence locations of relatively low resistivity (high conductivity) values are considered anomalous and are targeted for vertical electrical sounding. This is exemplified at distances 50, 180, 280 and 340 m in Figure 8a for VES4, VES3, VES2 and

VES1 respectively. These VES points coincide with anomalous zones identified on EM1 curves (Figure 9a) corresponding to station distance of 50, 400, 560 and 580 m for VES4, VES3, VES2 and VES1 respectively and are therefore expected to have moderately to thick overburden in their geoelectrical section.

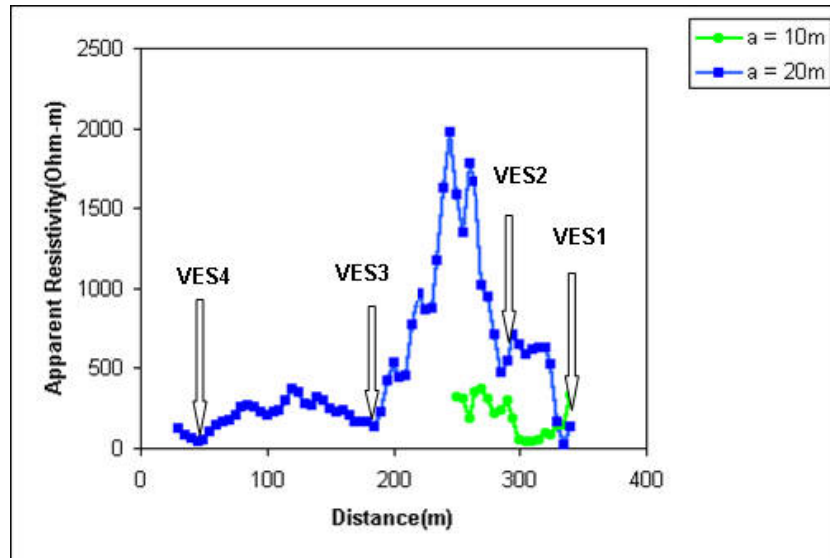


Figure 10a. Apparent Resistivity Profile R1 along E-W direction of the study area

In Figure 10b, the anomalously low resistive zone recommended for VES (VES10) is at distance mark of about 56 m and flanked by highly resistive zones on both sides which are probably made up of clayey sand/sand.

The horizontal electrical resistivity profile in Figure 10c has conductive zones between 40 m and 95 m mark, a lateral extent of about 55 m as prospective groundwater zone and delineated as VES5, VES6 and VES7 at about 42 m, 60 m and 78 m mark respectively.

The apparent electrical resistivity profile in Figure 10d fluctuates as distance increases and reached anomalously high and low values at about 60 m and 90 m mark respectively but steadily increases afterwards. The anomalously low resistivity value at 90 m mark could be prospected for groundwater and hence delineated as VES8.

#### 4.2.2 Vertical Electrical Sounding (VES)

The apparent resistivity curves plotted using the VES data obtained along respective profiles EM1/T1; T3; EM2/T2, T4; and EM3 are as shown in Figure 11a, Figure 11b, Figure 11c and Figure 11d. The corresponding correlated geoelectric sections are as depicted respectively on Figure 12a, Figure 12b, Figure 12c and Figure 12d. The geoelectrical succession comprises three to five layers and show variations in thickness of the weathered layer both along the same profile and over the entire area.

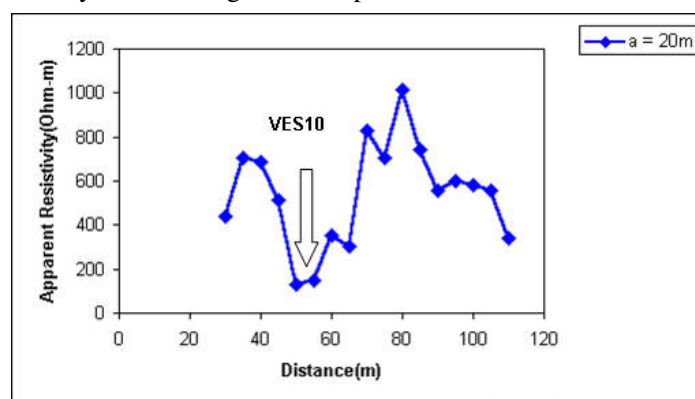


Figure 10b. Apparent Resistivity Profile R2 along E-W direction of the study area

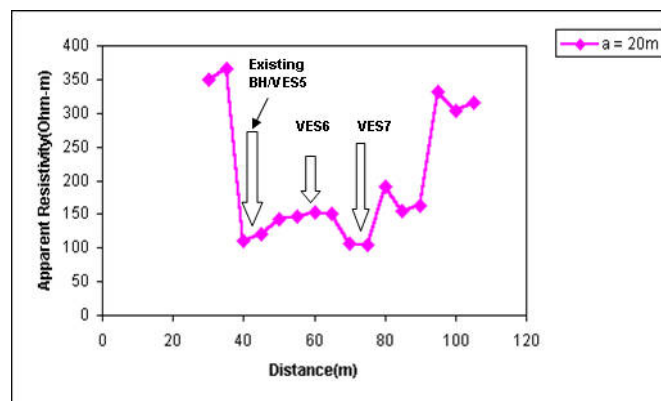


Figure 10c. Apparent Resistivity Profile R3 along E-W direction of the study area

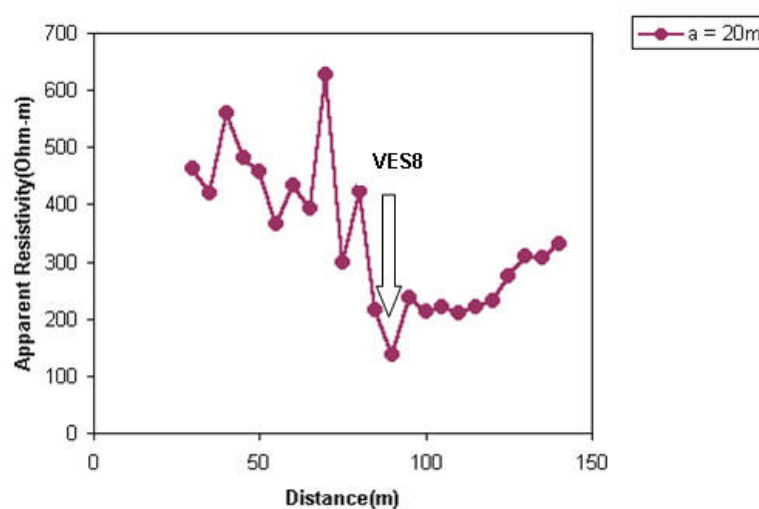


Figure 10d. Apparent Resistivity Profile R4 along E-W direction of the study area

Along the geo-electric section for profiles EM1 and T1 (Figure 12a) comprising VES1, VES2, VES3 and VES4 (Figure 11a); the topmost layer ranged from 0.5 m to 2.0 m in thickness with varied resistivity values between 62  $\Omega\text{m}$  and 1056  $\Omega\text{m}$ . The thickness of the weathered layer ranged from 0.8 m to 10.0 m with resistivity values between 10  $\Omega\text{m}$  and 90  $\Omega\text{m}$ . The average thickness of 6 m along this profile suggests that the overburden is shallow. It is however possible that the basement is faulted in places considering the repeated sequence of clay and clayey sand layer in vertical succession as indicated by their resistivity values (<10 - 100  $\Omega\text{m}$  for clays/sandy clay and 100 - 200  $\Omega\text{m}$  for clayey sand) at VES2. Consequently, the geo-electric signatures of the VES points vary and indicate variation in electrical properties of the subsurface layering sequence. Whilst VES1 and VES3 depicts four-layer *resistive – conductive – resistive – resistive* sequence (*HA-type* apparent resistivity curve) geo-electric signature indicating probable shallow overburden, VES2 and VES4 exhibit four-layer *resistive-conductive-resistive-conductive* sequence (*HK-type* apparent resistivity curve) and *conductive-resistive-conductive-resistive* sequence (*KH-type* apparent resistivity curve) respectively with preponderance of clay/sandy clay/clayey sand in the conductive zone.

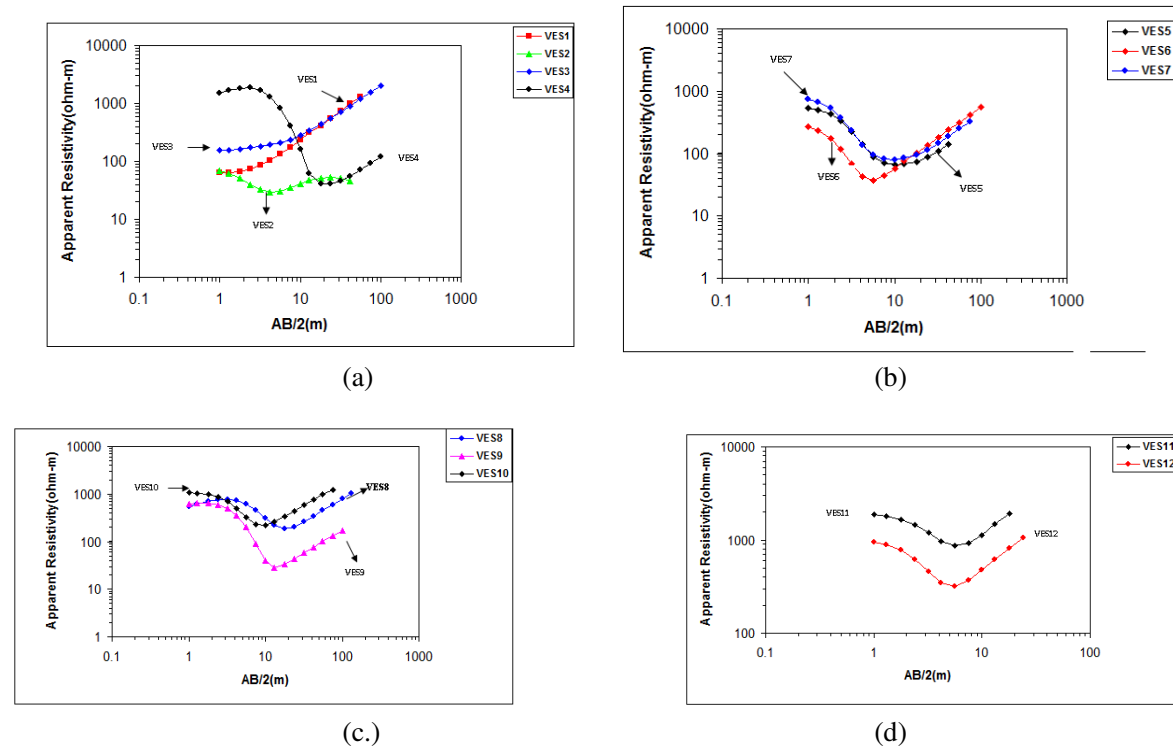


Figure 11. Vertical Electrical Sounding (VES) curves of the study area. (a) VES curves along profile EM1/T1, (b) VES curves along profile T3, (c) VES curves along profiles EM2/T2 and T4, (d) VES curves along profile EM3

Along electrical resistivity profile T3; the geo-electric section (Figure 12b) comprising VES5, VES6 and VES7 indicate a topmost layer having a thickness of about 1 m with resistivity value of 300  $\Omega\text{m}$  to 800  $\Omega\text{m}$ . The weathered layer is rather thick and clayey with resistivity values between 20  $\Omega\text{m}$  and 80  $\Omega\text{m}$  having average thickness of 15 m. The geo-electric signature in this location is predominantly three-layer sequence of *resistive-conductive-resistive (H-type)*, (Figure 11b) with the conductive layer as the water saturation zone. The basement resistivity value of 998  $\Omega\text{m}$  at VES5 is an indication of fractured basement (Verma *et al.* 1980; Hazell *et al.* 1988; White *et al.* 1988; Langenheim *et al.* 2000; Adabaniya *et al.*, 2008).

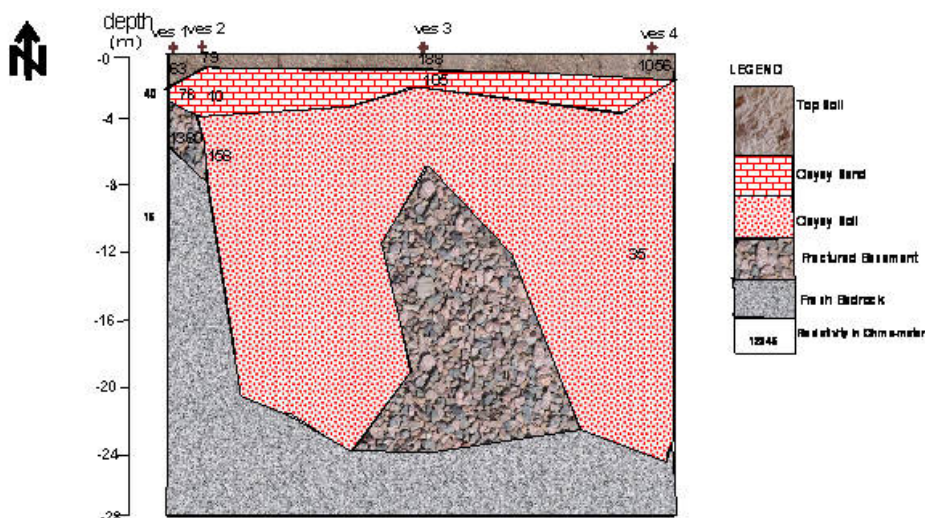


Figure 12a. Correlated geo-electric section along profile EM1/T1

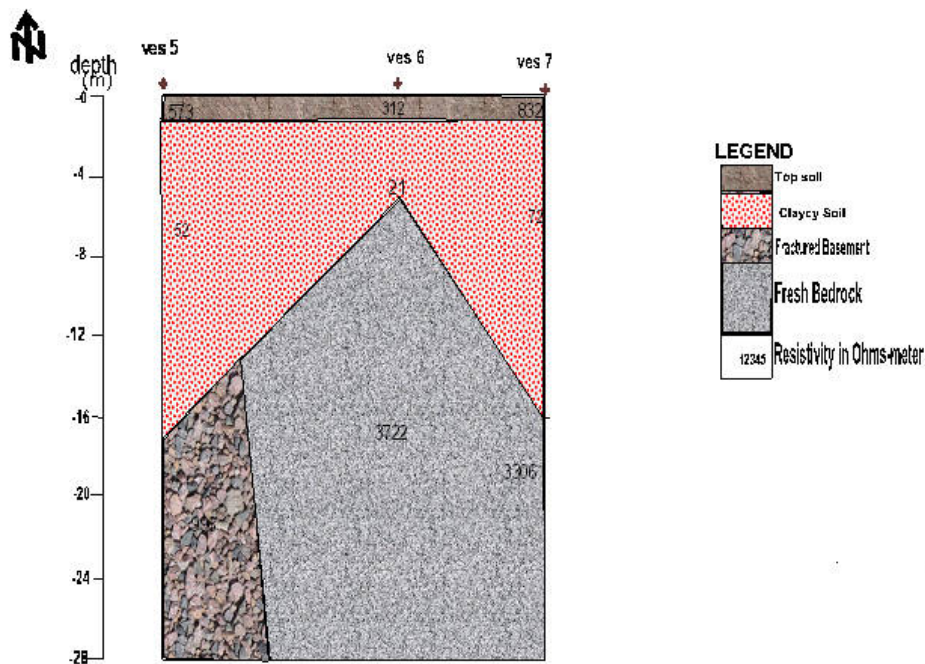


Figure 12b. Correlated geo-electric section along profile T3

The geo-electric section (Figure 12c) along profile EM2/T2 made up of VES9 and VES10 (Figure 11c) shows similar sequence to profile EM1/R1 with topmost layer having average thickness of 1 m and resistivity values ranging between 500  $\Omega$ m and 1000  $\Omega$ m. The weathered layer is clayey with resistivity values between 10  $\Omega$ m and 100  $\Omega$ m having average thickness of 8 m. The overburden here is relatively thick but clayey. Hence, a good development of aquifer system would have to rely on the fractured basement, as clays are poor aquifers except where they act as confining beds.

The geo-electric section (Figure 12d) of VES11 and VES12 indicates a system of 3-layer earth model having *resistive-conductive-resistive* (H-type) geoelectrical succession. The conductive zone is made up of clayey sand/weathered material and underlain by highly resistive fresh basement.

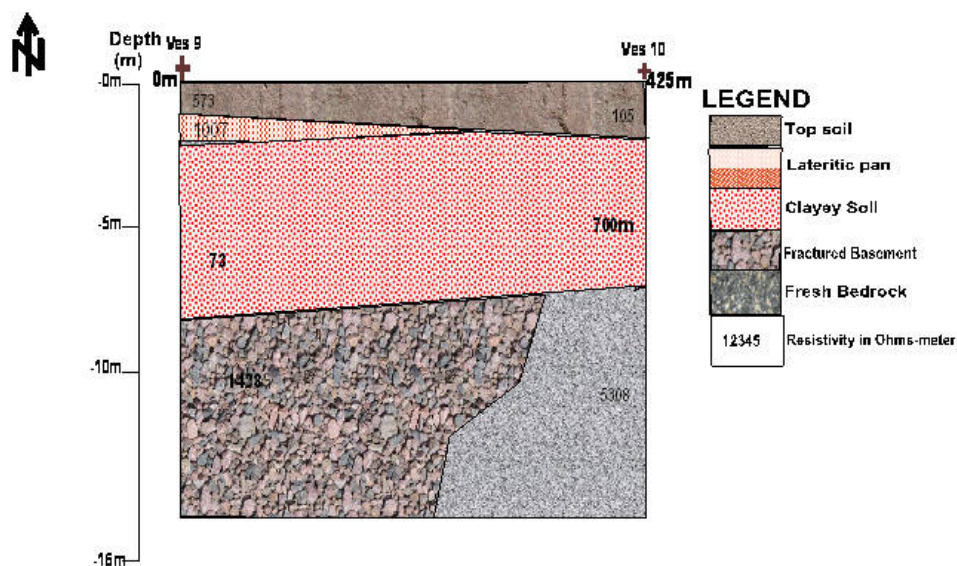


Figure 12c. Correlated geo-electric section along profiles EM2/T2 and T4

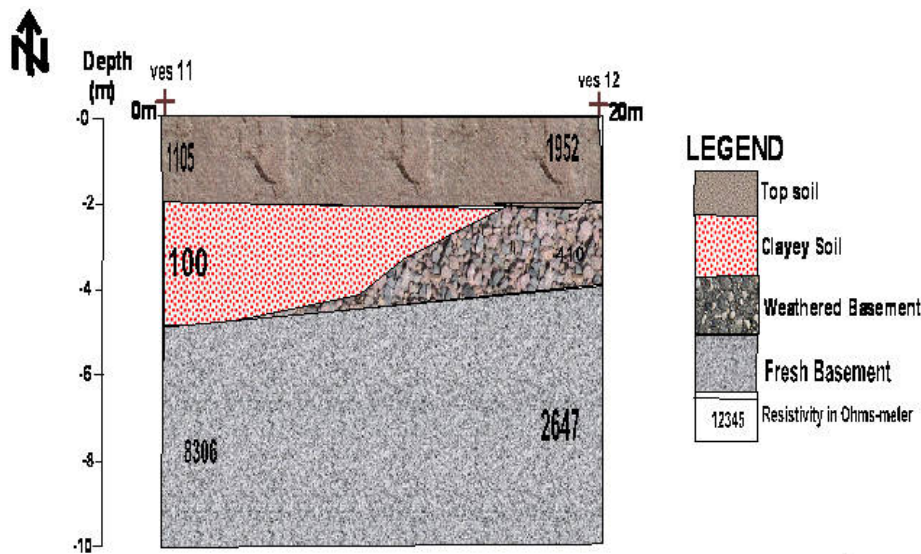


Figure 12d. Correlated geo-electric section along profile EM3

#### 4.3 Description of Borehole logs

The drillers log descriptions based on in-situ analysis of drill cuttings obtained from the three bore wells drilled at three VES points are as on Tables 1 to 3.

##### Well - A

Well-A was bored along profile T4 around VES8 which geoelectric signature is as depicted on Figure 11c. Its lithologic profile as inferred from Table 1 indicates weathered granitic rock between 55 – 80 ft and multiple fractures from 80 – 120 ft. This corroborates the geoelectric signature which exhibits a five-layer sequence of *conductive-resistive-conductive-resistive* (KHA-type) with the last three layers displaying ascending type behavior indicating increase in resistivity with depth and is as corroborated by thickening of coarse material towards the partly weathered (fracture) saprolite overlying the basement. Draw-down and yield test indicated the well is capable of producing water at a rate of 590.4LPH or 14169.6l/day

Table 1. Lithologic description of cuttings from Well A with depth

Depth (ft)	Lithologic Description
0 – 5	Top soil
5 - 35	The cuttings were weathered and the grains were coarse. The major minerals present include feldspar, biotite, quartz with respective probable percentage composition as: 60%, 30% and 10% indicating granite.
35 - 45	Same as in 5 – 35ft column but there was an increase in percentage composition of biotite (45%) and quartz (15%) while the quantity of feldspar decreases (40%). The composition is still granitic.
45 – 55	The cuttings were fresher than those at the overlying column. Mafic composition was greater than the felsic content. The percentage of biotite at this depth is probably about 60%, 20% feldspar, and 20% quartz. The sample is granite.
55 – 65	The cuttings appeared to have undergone weathering as a result of reduction in the percentage of biotite (50%). However, there was more feldspar (30%) while the percentage of quartz was unchanged (20%)
65 – 80	At this interval, there was combination of weathered (about 70%) and fresh (about 30%) sample. The percentage of dominant minerals were biotite 40%, feldspar 40% and quartz 20%
80 – 90	Some of the cuttings were fresh while some of them have brownish stain which must have been as a result of close contact between that part of the rock and water. This depth can therefore be regarded as fractured and contain water that tends to aid the weathering of some part of the rock. Mineralogically, the cuttings contain biotite (50%), feldspar (35%) and quartz (15%) indicating equal percentage composition of both mafic and leucocratic minerals. The composition still indicates granite.
90 – 100	The cuttings are smaller in size than those in 80 – 90ft interval and are highly weathered. They contain more feldspar and quartz and must have been derived from a fracture zone which contains water that aided the weathering of the rock at that area and consequently rendered it brittle. Hence, the cuttings were crushed into smaller sizes by the drilling hammer. Some of the feldspar

	cuttings contain some digested biotite suggesting quartzo- feldsparthic vein intrusion into the granitic rock. The mineralogical composition could therefore be of the order feldspar >quartz>biotite.
100 – 110	The cuttings though larger in size than those in 90 – 100ft column still appeared weathered and very close to fracture zone and quartzo-feldsparthic vein. The sample is still granitic having the same order of percentage composition of feldspar, quartz and biotite as in 90 – 100 ft interval but more felsic.
110 – 120	Cuttings are larger and material compositions are more felsic than mafic. The surfaces of some of the cuttings indicate stains of weathering which must have been caused by the water that percolates into the fracture. This zone is thus a highly fractured granite interval.

**Well - B**

Well-B was drilled around VES2 along profiles EM1 and T1. The lithologic profile as deduced from Table 2 was in strong agreement with the *resistive-conductive-resistive-conductive* geoelectric sequence of VES2. The first conductive zone is as indicated by the interval 0 – 18 ft comprising conductive clay and highly weathered rock material (Table 2). This was followed by the interval 18 – 78 ft made up mainly of fresh rock cuttings (Table 2) and usually electrically resistive (Adabanija *et al.*, 2008). This was underlain by conductive zone corresponding to interval 78 – 105 ft (Table 2) comprising fracture and highly weathered unit. Draw-down and yield test indicated the well is capable of producing water at a rate of 520.8LPH or 12,499l/day

Table 2. Lithologic description of cuttings from Well B with depth

Depth (ft)	Lithologic Description
0 – 3	Lateritic pan/ Indurated laterite fragments, quartz and feldspar
3 – 9	Clayey sand/clayey laterite made of feldspar, quartz and indurated/lateritic pan grains held together by the clay materials.
9 – 18	Highly weathered rock materials having quartz, feldspar and biotite of different grain sizes.
18 – 27	Fresh rock cuttings made up of feldspar, quartz, biotite and other mafic minerals. Rock must have been a gneiss containing minerals in the order of percentage composition mafic minerals > feldspar > quartz indicating gneiss.
27 – 54	Very fine grain, biotite and quartz grain well. The fineness must have been due to grinding by the drilling hammer prior to flushing out of the hole.
54 – 69	Cuttings were of larger size comprising biotite, feldspar and quartz with quartz and biotite in equal proportion.
69 – 78	Same as in interval 54 – 69 ft
78 – 90	The cuttings were very large having mineral bandings of felsic and mafic minerals in about equal proportion though without feldspar. Some of the cuttings were partially weathered. The large size of the cuttings and their partial weathering appearance depicts a fracture zone.
90 – 105	Highly weathered large quartz grains cuttings with no indication of biotite. Some of them have small patches around their surfaces. Thus the interval must have been a weathered quartzo-feldsparthic vein serving as reservoir for the percolating and subsurface water.

**Well-C**

Well-C was spudded around VES11 along profile EM3. The lithologic profile (Table 3) indicates the interval 0 – 10 ft to be made up of lateritic clay and usually electrically resistive. The conductive zone spans the interval 10 – 60 ft comprising clay and intensely weathered material (Table 3) and constitutes the aquifer units of the hole. Decrease in feldspar composition beyond 60 ft (Table 3) indicates decrease in clay content and hence increase in resistivity (Olayinka, 1992). Thus there is strong agreement between the geoelectric succession of VES11 and the lithological profile. The yield of the hole as obtained from draw-down and yield test indicates 280.6LPH or 6,734.4l/day.

Table 3. Lithologic description of cuttings from Well C with depth

Depth (ft)	Lithologic Description
0 – 10	Lateritic clay – reddish in colour
10 – 20	Clayey sand; Clay-40%, Sand 60%
20 – 30	Pebbles of quartz, feldspar and lateritic pan which must have been derived from intense weathering. The quartz grains have a brownish/reddish colour stain. The sample contains about 50% quartz, 40% lateritic pan and 10% feldspar grains. The grains are large.
30 – 40	Sample still contain quartz, feldspar and fragments of indurated laterite/lateritic pan. The probable composition is Feldspar 50%, quartz 30% and indurated laterite 20%
40 – 50	Same as in preceding interval but pebbles/cuttings are smaller in size and have an increase amount of feldspar grains.
50 – 60	Same as in interval 40ft – 50ft
60 – 70	Same as in interval 40ft – 50ft but with reduced amount of feldspar grains.

## 5.0 Conclusions

VLF-EM profiling and Electrical Resistivity methods have been used to explore the aquifers and characterize hydro-geologic conditions of a low latitude basement complex in Ogbomoso North. The aquifers are made up of fractured and highly weathered rock units and which are localized in nature. The lowest yield of 380.6LPH was obtained from well bored on VES point having 3-layers earth model (*resistive-conductive-resistive*) geoelectrical succession. Well bored on VES points having more than 3-layers earth models and comprising alternating band of *resistive-conductive* geoelectric succession have more yield ranging between 520.8LPH and 590.4LPH. The study also revealed strong agreement between geoelectric successions and lithologic profiles obtained from the drill cuttings of the bored wells. However, there was no correlation between the thickness of the layers obtained from quantitative interpretation of the apparent resistivity curves and the intervals on the lithological profile.

## References

- Adabanija, M. A., Omidiora, E. O., Olayinka, A. I., (2008). Fuzzy logic modeling of the resistivity sounding measurement and topography features for aquifer assessment in hydrogeological investigation of basement complex. *Hydrogeol. Journal* 16(3):461-481
- Afolabi, O. A., Kolawole, L. L., Abimbola, A. F., Olatunji, A. S., Ajibade, O. M., (2013). Preliminary Study of the Geology and Structural Trends of Lower Proterozoic Basement rocks in Ogbomoso, SW Nigeria. *Journal of Environment and Earth Science*, Vol. 3, No. 8, pg. 82-95
- Amadi, U. M. P., Nurudeen, S. I., (1990). Electromagnetic survey and the search for groundwater in the crystalline basement complex of Nigeria. *Jour. Min. Geol.*, 26 (1): 45-55.
- Benson, S., Jones, C. R. C., (1988). The combined EMT/VES geophysical method for siting boreholes. *Ground Water*, 26: 45-63
- Jones, H. A., Hockey, R. D., (1964). Geology of part of southwestern Nigeria. *Geological survey of Nigeria bulletin*, 31: 25pp.
- Ghosh, D. P., (1971). Inverse filter coefficients for the computation of apparent resistivity standard curves for a horizontal stratified earth. *Geophysical Prospecting*, 19: 769-775.
- Goldman, M., Rabinovich, B., Rabinovich, M., Gilad, D., Gev, I., Shirov, M., (1994). Application of the integrated NMR-TDEM method in groundwater exploration in Isreal. *Journal of Applied Geophy.* 31: 27-52.
- Hazel, J. R. T., Crachley, C. R., Preston, A. M., (1988). The location of aquifer in crystalline rocks and alluvium in northern Nigeria using combined electromagnetic and resistivity techniques, *Quarterly Jour.*

*Eng. Geol.*, 21:159-175.

Jones, M. J., (1985). The weathered zone aquifers of the Basement complex areas of Africa. *Quarterly Journal of Eng. Geology*, 18: 35-46

Jones, C. R. C., Beeson, S., (1985). The EM/VES Geophysics technique for Borehole siting Kano State. In: *Oguntona, T. (ed.) Advances in Groundwater detection and extraction, Int. Conf. on Arid zone hydrology and water Resources, Maiduguri*

Klein, J., Lajoie, J., (1980). Electromagnetic Prospecting for minerals. Practical geophysics for the Exploration geologists. *Northwest Mining Association, Spokane, WA: 239 -290*

Langenheim, V. E., Glem, J. M., Jachens, R. C., Dixon, G. L., Katzer, T. C., Morin, R. L., (2000).

Geophysical constraints on the Virgin river depression, Nevada, Utah and Arizona. US department of Interior, US geological Survey open-file Report 00-407

McNeil, J. D., (1980a). Electromagnetic Terrain Conductivity Measurement at Low Induction Numbers, Technical Notes TN-6, TN-8, Ltd, Missiauga, Ontario.

McNeil, J. D., (1980b). EM 34-3 Survey Interpretation Techniques. Tech. Note TN- 8 (Rev. 1983)

McNeil, J. D., (1990). Use of electromagnetic methods for groundwater studies. *Geotechnical and environmental Geophysics*, 1: 191-218.

Olayinka, A. I., (1990). Electromagnetic profiling for groundwater in Precambrian basement complex areas of Nigeria. *Nordic Hydrology*, 21: 205-216.

Olorunfemi, M. O., (1990). Hydrogeological implication of topographic variation with overburden thickness in basement areas of southwestern Nigeria. *Jour. Min. Geol.*, 26(1): 145-152.

Olorunfemi, M. O., Ojo, J. S., Sonuga, F. A., Ajayi, O., Oladapo, M. I., (2000). Geoelectric and electromagnetic investigation of the failed Koza and Nassarawa earth dams around Katsina, Northern Nigeria. *Jour. Min. Geol.*, 36: 51-65.

Oyedele, K. F., Momoh, E. I., (2009). Evaluation of sea water intrusion in freshwater aquifers in a lagoon coast: A case study of the University of Lagos Lagoon Akoka Nigeria. *Report Opinion*, 1(2): 61 – 72

Palacky, G. J., Ritsema, I. L., De Jong, S. J., (1981). EM Prospecting for groundwater in Precambrian terrains in the Republic of Upper Volta (Burkina Faso). *Geophysical Prospecting*, 29: 932-955

Parasnis, D. S., (1990). Principles of Applied Geophysics, Chapman and Hall, London, fourth edition.

Payne, M. L., (1988). The electromagnetic traversing method of groundwater exploration in crystalline rock terrain (Thurber Environmental Consultants Ltd, Victoria Canada).

Reynolds, J. M., (1987). The role of surface geophysics in the assessment of regional groundwater potential in Northern Nigeria. In: *Culshaw MG, Bell FG and O'Hara (eds.), Planning and Engineering Geology. Geological Society London, Engineering Geology Special Publications*, 4:185-190

Verma, R. K., Rao, M. K., Rao, C. V., (1980). Resistivity Investigations for groundwater in metamorphic areas near Dhanbad, India. *Ground Water*, 18:46-55.

White, C. C., Houston, J. F. T., Barker, R. D., (1988). The Victoria Province Drought Relief Project, 1, Geophysical siting of bore-holes. *Ground Water*, 26:309-316.

Zohdy, A. A. R., Eaton, G. P., Mabey, D. R., (1974). Application of surface geophysics to techniques of water resources investigations Book 2, Chapter D.

This academic article was published by The International Institute for Science, Technology and Education (IISTE). The IISTE is a pioneer in the Open Access Publishing service based in the U.S. and Europe. The aim of the institute is Accelerating Global Knowledge Sharing.

More information about the publisher can be found in the IISTE's homepage:

<http://www.iiste.org>

## CALL FOR JOURNAL PAPERS

The IISTE is currently hosting more than 30 peer-reviewed academic journals and collaborating with academic institutions around the world. There's no deadline for submission. **Prospective authors of IISTE journals can find the submission instruction on the following page:** <http://www.iiste.org/journals/> The IISTE editorial team promises to review and publish all the qualified submissions in a **fast** manner. All the journals articles are available online to the readers all over the world without financial, legal, or technical barriers other than those inseparable from gaining access to the internet itself. Printed version of the journals is also available upon request of readers and authors.

## MORE RESOURCES

Book publication information: <http://www.iiste.org/book/>

Recent conferences: <http://www.iiste.org/conference/>

## IISTE Knowledge Sharing Partners

EBSCO, Index Copernicus, Ulrich's Periodicals Directory, JournalTOCS, PKP Open Archives Harvester, Bielefeld Academic Search Engine, Elektronische Zeitschriftenbibliothek EZB, Open J-Gate, OCLC WorldCat, Universe Digital Library, NewJour, Google Scholar

